A Modification on ECAP Process by Incorporating Twist Channel

Hosein Bisadi, Mehdi Rezazadeh Mohamadi, Hadi Miyanaji, and Maryam Abdoli

In this study, a method that combines the equal channel angular pressing (ECAP) and twist extrusion (TE) techniques has been introduced as a severe plastic deformation process and investigated by means of the three-dimensional finite element analysis. Owing to the form of the mold which is used in this technique, it can be called the symmetrical channels angular pressing (SCAP) method. This method resembles the more common ECAP process for samples with rectangular cross sections, with the difference that, in this method, the entrance and exit channels at the intersecting corner of the mold also have a twist about their longitudinal axis (as in the TE technique). In this study, to show the characteristics of the SCAP method and to compare it with the ECAP technique, the former method has been simulated by the ABAQUS/Explicit software. Also, to validate the obtained results, the SCAP and ECAP methods were practically applied on samples made of pure commercial aluminum (AA1050). To get the strain distribution along the longitudinal and transverse directions of the samples, Vickers hardness was measured on these samples. The results obtained from these hardness measurements indicate that after one pass, the SCAP method can achieve a higher amount of hardness, compared with the ECAP technique. Moreover, the strain distributions obtained from the simulation and from the samples demonstrate that the SCAP method produces a more homogeneous distribution of strain in the workpieces.

1. Introduction

Severe plastic deformation (SPD) methods are processes in which very high plastic strains are applied to materials. The difference between these methods and the common forming techniques is that, after the application of strain to the samples undergoing the process, the sample's final dimensions remain unchanged. This makes the process repeatable for many times, and as a result of this repetition, strain accumulates in the samples, causing the density of dislocations to increase, and finally resulting in the production of very fine-grained, and even nanostructure materials (Ref 1). Because of their microstructure and unique grain sizes, these materials have special physical and mechanical properties. In recent years, different methods of SPD have been proposed including the equal channel angular pressing (ECAP) (Ref 2), high-pressure torsion (HPT) (Ref 3), multiaxial compressions/forging (MAC/F) (Ref 4), and twist extrusion (TE) (Ref 5) for bulk materials, and the constrained groove pressing (CGP) (Ref 6) and accumulative roll bonding (ARB) (Ref 7) techniques for sheet materials. In order to attain the desired outcome, all these methods should go through repeated passes, prolonging the process and making it costlier. To overcome this problem, these methods could be combined with one another or with other forming techniques, so that in each pass, a more effective stain is achieved. For the merging of the above methods, some approaches such as the torsional ECAP (Ref 8), dual equal channel lateral extrusion (DECLE) (Ref 9), multipass ECAP (Ref 10), and the torsion extrusion (Ref 11) have been tried. It can be said that, from among the many SPD processes, the ECAP method has a better chance of becoming industrialized because of its success in the production of fine-grain materials and large size parts, and because it requires simple equipment to accomplish the task. The TE method is another SPD process, which has been studied in a number of cases, and has been successful in producing ultra-fine-grain materials (Ref 5, 12-14). The TE process also has special characteristics and advantages, relative to the ECAP process. For example, the vortex Flow that exists in the TE process causes the metal particles to be drawn out and stretched. The degree of stretching increases with the increasing number of TE passes. Successive passes, accompanied by change of rotation direction, cause the stretched bands to fold repeatedly, and ultimately result in the mixing and fine graining of the particles (Ref 5). This material-mixing capability of the TE process is one of its prominent features, which can be used in the homogenization of composite materials. Moreover, it has been already demonstrated that simple shear is the optimum deformation mode for the development of spatial networks of high angle boundaries and fine grains in the course of local flow for monotonic and cross loading (Ref 15). Therefore, additional planes with simple shear strain can assist in the fine graining of material structure. The deformation mode in the TE process is simple shear. Two planes are perpendicular to the extrusion axis, and two planes are parallel to the extrusion axis, which is different from the shear plane in the ECAP process. In addition, in the TE process,

Hosein Bisadi, Mehdi Rezazadeh Mohamadi, Hadi Miyanaji, and **Maryam Abdoli**, Department of Mechanical Engineering, Iran University of Science & Technology, Tehran, Islamic Republic of Iran. Contact e-mail: rezazadeh.mrm@gmail.com.

the advantages of the strain gradient can also be benefitted (Ref 5). By combining the two methods of ECAP and TE, the advantages of both techniques can be exploited simultaneously. Kocich et al. (Ref 16) performed experiments on pure copper by placing the outlet of the TE mold into the inlet of the ECAP mold. In this article, the methods of TE and ECAP are merged with each other in the intersecting corner of the mold. This combination increases the applied strain and creates different routes for repeated passes of the sample. For the two methods of symmetrical channels angular pressing (SCAP) and ECAP, the results obtained from the finite element simulation and from practical experiments, with respect to the amount and distribution of applied effective strain, applied force, and the amount and distribution of hardness, have been compared with one another.

2. General Principles of the Method

The principles of the SCAP method are generally similar to those of the ECAP, with the difference that the two end section channels that meet each other are not straight and the passageway with the constant cross section goes through a twist. In fact, the route through which the sample passes inside the mold (as seen in Fig. 1) can be described as follows. The inlet section of the mold has a straight path with the same cross section as that of the sample. After going through the inlet section, the sample enters the twisted section of the passageway. The outlet section of the mold is symmetrical to the inlet section, relative to the shear plane with arbitrary angle; this angle is one of the significant parameters of the process. The sample's cross section remains unaltered after completely passing through the mold; thus, the process can be repeated many times and by doing so, effective strain can be accumulated in the sample. The influential parameters in this process are the four angles of ψ, ϕ, α, and β. As shown in Fig. 1, the angles of ψ and ϕ (like in the ECAP process) are the angles between the inlet and outlet channel axes, and the bend angle of the mold's corner, respectively. Angle β is the twist angle, and α is the amount of rotation of the outlet cross section relative to the inlet cross section.

Because of the particular structure and shape of the mold, the twisting and turning directions of the sample during entrance and exit are opposite to each other; meaning that the workpiece twists about its axis in a clockwise direction as it enters the mold, and in a counter-clockwise direction as it exits
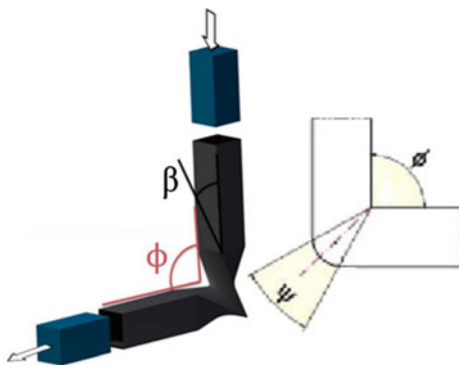

Fig. 1 Schematic representation of the SCAP process

the mold, or vice versa. Therefore, in the course of different passes, the sample can be forced through the mold in different routes, which will cause different material structures and properties to be produced. As shown in Fig. 2, the sample can be passed through the mold in eight different ways. These eight manners include the methods of *A*, *BA*, *BC*, and *C*, in the form of simple, and alternating turns. The methods of *A*, *BA*, *BC*, and *C* are different routes of passing the samples in the ECAP process. If the samples enter the mold from one inlet during all the passes, then the simple method of (*C*) is obtained, and if the samples' inlet changes alternately, then the alternate method of (*A*) is achieved. Of course, instead of changing the inlet, the sample can be rotated 180° about an axis perpendicular to the extrusion axis.

3. Experimental Procedure

The mold used in the SCAP process (as shown in Fig. 3) consists of four sections. The twisted sections of the mold are two separate parts which are fitted with the parts that form the inlet and outlet routes, and together, they make up the passageway of the sample. In the used mold, angles ϕ, ψ, and β are 90°, 0°, and 15°, respectively. Angle α (i.e., the amount of rotation of the outlet cross section relative to the inlet cross section) is equal to 90°. Angles ϕ and ψ are also 90° and 0° in the mold used for the ECAP process, respectively.

The samples used in both methods have cross sections of 20×20 mm and length of 100 mm. These samples are made of commercially pure aluminum (AA 1050) with the chemical composition (Si:0.25%, Fe:0.4%, Cu:0.05%, Mn:0.05%, Zn:0.05%, Mg:0.05%, Ti:0.03%, and Al:Rem) in wt.%, and are machined out of thick AA 1050 plates. To reduce defects and obtain materials with homogeneous properties, the samples are annealed in a furnace at the temperature of 500 °C for 2 h, and then cooled to room temperature. The SCAP process is carried out at room temperature by using a hydraulic press operating at a ramming speed of 1 mm/s. High-pressure grease is applied to reduce the friction between the sample and mold. To eject a sample out of the mold, the next sample which is fed into the mold to undergo the process can be used. For comparison between SCAP and ECAP, samples are passed through the molds with one pass, and then they are prepared for Vickers hardness measurement.

The Vickers hardness is measured on two planes: one, normal to the extrusion axis and the other one, parallel to it. The hardness tests were performed by means of 100 gf load and 15-s dwell time. For the plane perpendicular to the extrusion axis, the Vickers hardness is measured along the lines *AB* and *CD*; and for the plane parallel to the extrusion axis, it is measured along the line *EF*, which is shown in Fig. 4.

3.1 Finite Element Simulation Procedure

To investigate the characteristics and behavior of the material during deformation, the commercially available finite element code ''ABAQUS/Explicit'' has been used. To be able to compare the results obtained from the simulation and the actual experiment, the sizes and dimensions of the mold and sample have been simulated exactly as they are in the actual process. The simulation has been performed in 3D form, and the stress-strain relation $\sigma = 106\varepsilon^{0.345}$ (obtained through the
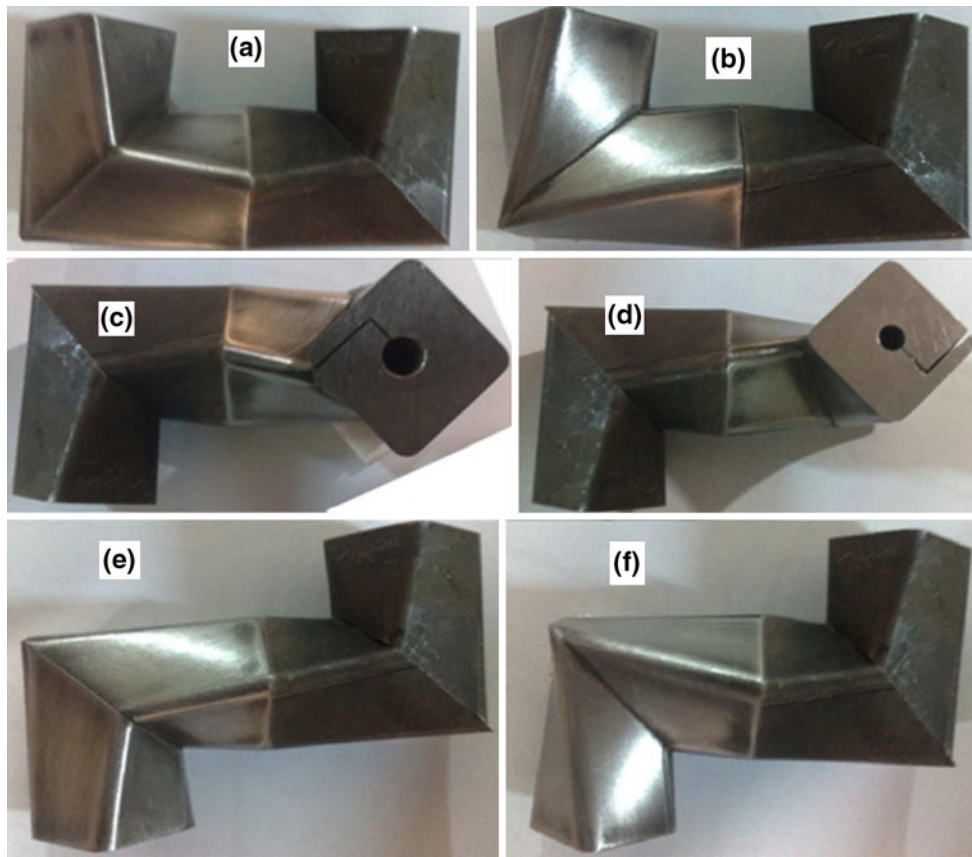
Fig. 2 Routes of SCAP in successive passes: (a) A_A; (b) A_A; (c) B_{AC} and B_{AA}; (d) B_{CC} and B_{CA}; (e) C_C; (f) C_A
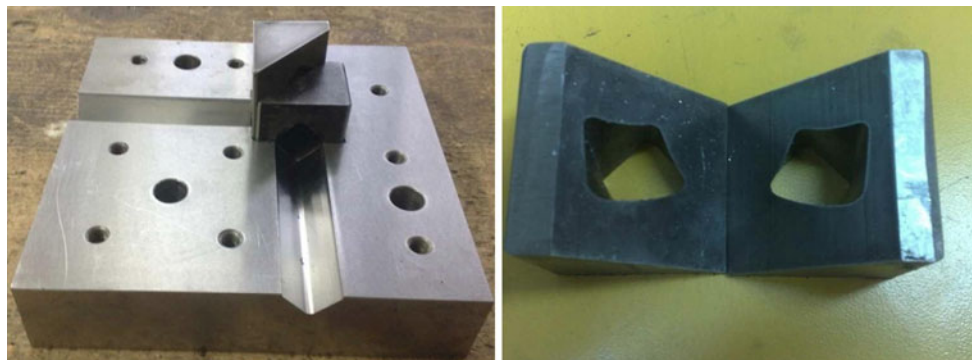

Fig. 3 A picture of the mold used in the SCAP process

compression test at ambient temperature) has been used. In view of the test conditions, the friction factor $m = 0.1$ (obtained from the barrel test) has been considered for the interfaces of mold and sample; using this value in relation (1), the friction coefficient has been obtained as $\mu = 0.2$ (Ref 17).

$$\mu = \frac{m}{\sqrt{27(1 - m^2)}} \qquad (\text{Eq 1})$$

To apply a mesh configuration to the billet and rigid parts, the linear 8-node elements (C3D8R) and four-node 3D bilinear rigid quadrilateral elements were used (Ref 18).

4. Results and Discussion

4.1 Comparison of the ECAP and SCAP Methods

As was stated in the previous sections, the SCAP process is similar to the ECAP process, except that in the SCAP method, in the intersecting part of the mold (where the material bends and undergoes shear strain), the two connecting channels have a twist about their longitudinal axes, and the direction of twist of the inlet channel is opposite to that of the outlet channel.

Figure 5 shows the load-displacement curves for the SCAP and ECAP processes. As is observed, the magnitude of the
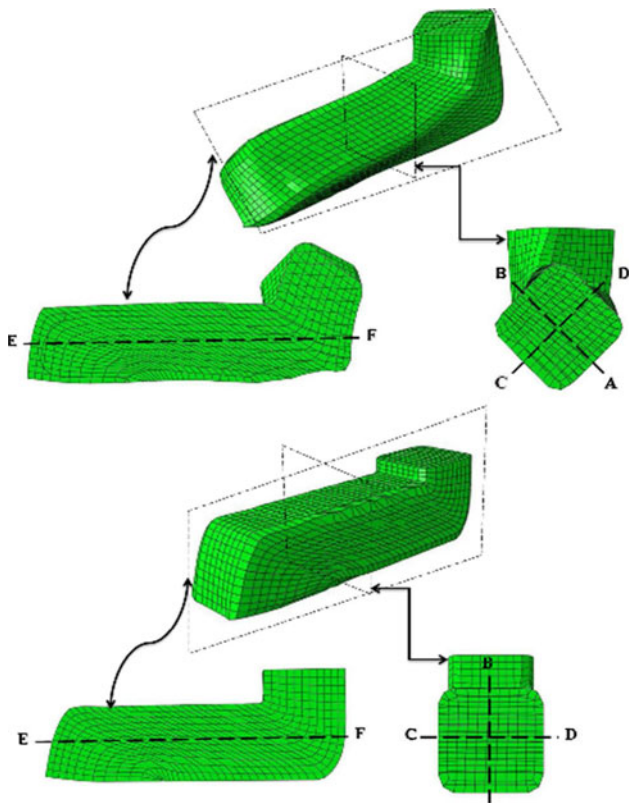
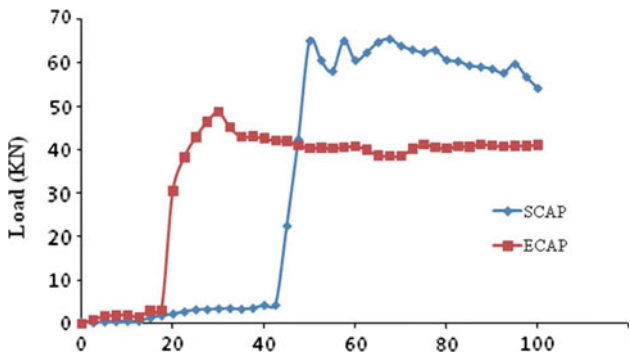**Fig. 4** Measurement points for hardness and effective strain

Fig. 5 Experimental load-displacement of the SCAP and ECAP processes

applied load for the SCAP is almost 30% more than that for the ECAP. This is because of the existence of twisted sections in the mold. As seen in Fig. 1, in order for the sample to pass through the mold, it should first traverse the twisted section of the inlet channel; hence, the applied load gradually increases until the sample reaches the intersecting section of the two channels. When the sample reaches the location where shear strain is imposed, the applied load increases abruptly. After passing through this section, the sample enters the twisted section of the outlet channel, and again a higher load is needed (relative to the ECAP which has straight passageways) to force the sample through this section. Once the sample passes through both twisted sections, the applied load assumes a stable and uniform state (same as in the ECAP process). Figure 6 shows the load-displacement diagrams obtained from the
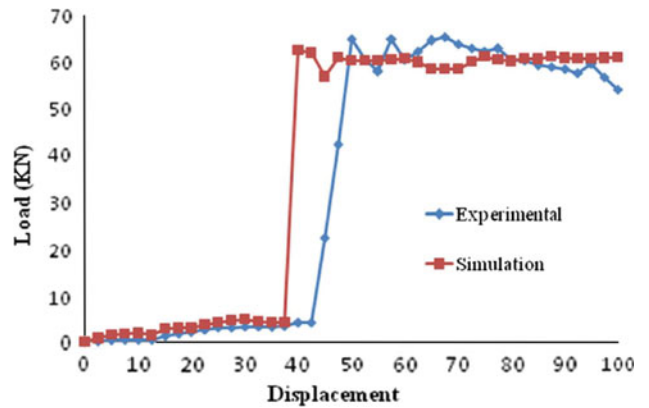

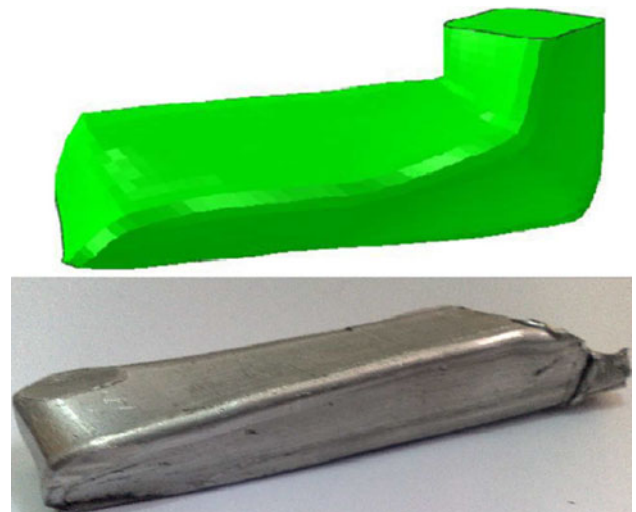**Fig. 6** Experimental and simulation load-displacement curve of the SCAP process

Fig. 7 The experimental and simulation-predicted deformed sample shapes

simulation and practical experiment. As the figure demonstrates, there is adequate correlation between the experimental and simulation results. The above explanations are also valid for the simulation results.

Figure 7 illustrates the deformed sample obtained from the practical experiment and also the final shape of the workpiece, which is predicted by the finite element method. As can be observed, both samples have identical shapes, and there is good agreement between the experimental and simulation results.

4.2 Hardness and Strain

As has been indicated in Fig. 4, the hardness of the sample is measured along the lines *AB*, *CD*, and *EF* on planes that are parallel and perpendicular to the extrusion axis. These planes have been selected in consideration of the applied strains in the SCAP process; and It should be noted that the selection of these sections was based on the microstructural change in the ECAP process, as reported by Iwahashi et al. (Ref 8), as in these sections, different microstructure were expected. Figure 8 shows the effective strains obtained from the simulation, and also the hardness values measured along the lines *AB*, *CD*, and *EF* for the ECAP and SCAP processes. Figure 8(a) illustrates
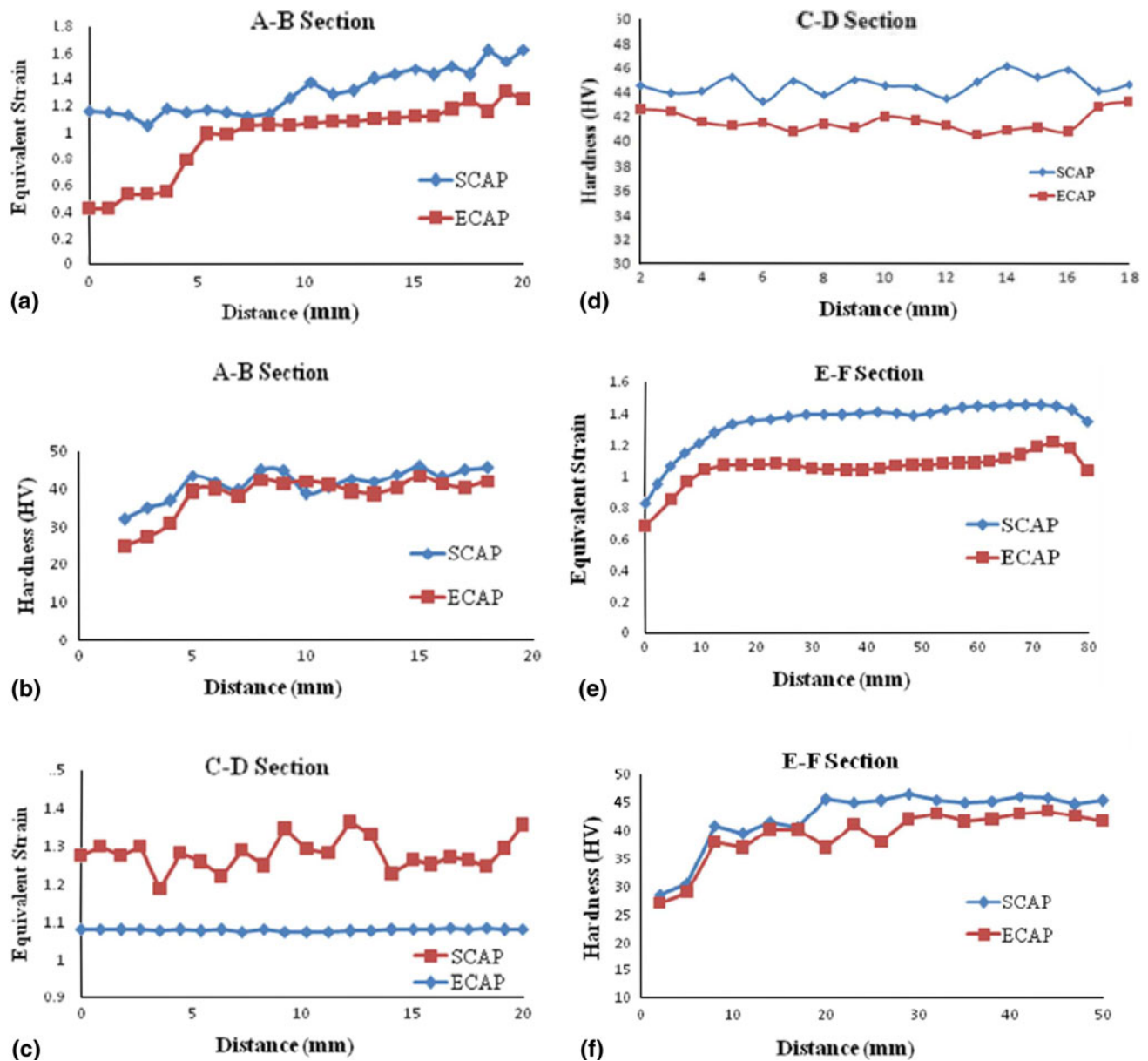
Fig. 8 Distribution of simulation strain and experimental hardness of SCAP and ECAP sample, (a) strain, section *A-B*; (b) hardness, section *A-B*; (c) strain, section *C-D*; (d) hardness, section *C-D*; (e) strain, section *E-F*; (f) hardness, section *E-F*

the effective strain distribution along the *AB*. In the ECAP method, strain has its lowest value at point *A* (bottom part of the mold), and by moving toward point *B* (top part of the mold), the amount of strain increases. The formation of a dead zone or empty space in the corner of the mold is the cause of this phenomenon, which occurs more frequently for materials showing a strain hardening (Ref 19). However, in the SCAP process, the resulting strain not only has a higher value at every point, but also has a more uniform distribution. This phenomenon is due to the manner in which strain is imposed on the material in the ECAP and TE processes. In the ECAP method, the applied strain mostly affects the center of the sample, while in the TE method, most of the strain is applied to the sample's exterior surfaces, and the center of the sample undergoes the least amount of strain. Therefore, by combining these two

processes, a more uniform effective strain can be achieved in the sample.

As shown in Fig. 8(c), the effective strain obtained in the ECAP process along the line *CD* has an almost uniform distribution, which can be justified by the fact that the ECAP process creates plane strain in rectangular samples. The amount of this strain is obtained from relation (2) (Ref 20).

$$\varepsilon = \frac{1}{\sqrt{3}}\left[2\cot\left(\frac{\psi}{2}+\frac{\phi}{2}\right)+\psi\,\mathrm{cosec}\left(\frac{\psi}{2}+\frac{\phi}{2}\right)\right] \qquad \text{(Eq 2)}$$

In the above relation, ϕ is the angle of intersection of the two channels, and ψ is angle of curvature used for the mold. For the ECAP process, these angles are 90° and 0°, respectively. These parameter values result in an effective strain value of 1.15 at every pass, which is also similar to the
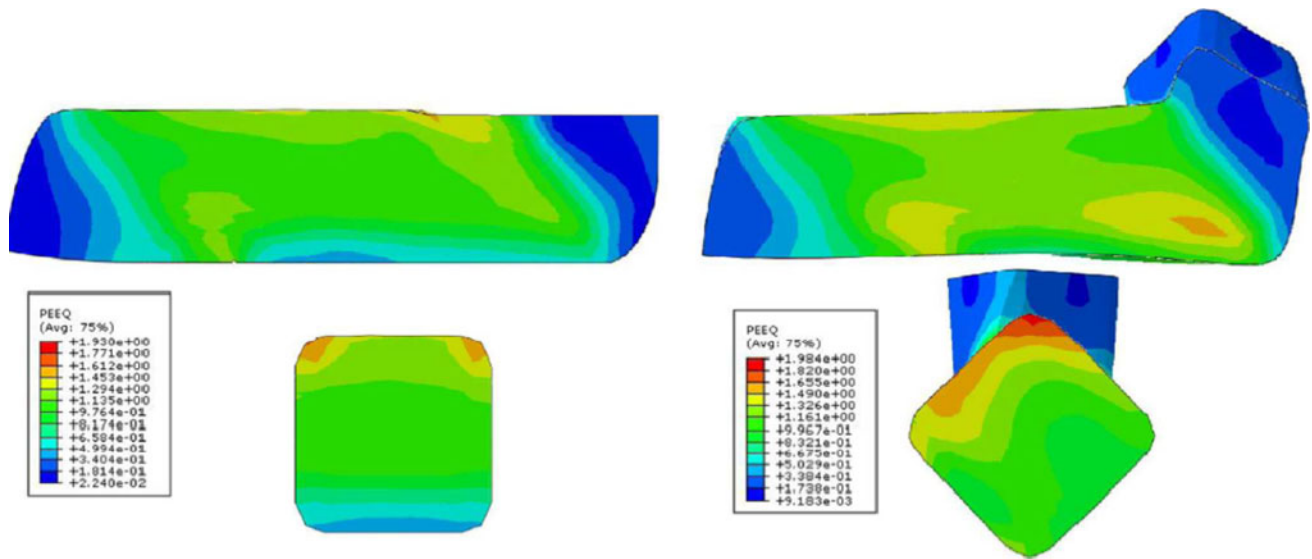
Fig. 9 Strain contour on longitudinal and transverse sections of ECAP and SCAP samples

results obtained from the simulation. Also, the obtained strain for the SCAP process enjoys similar uniformity along the lines *CD* as well as *AB*.

The distribution of effective strain along the *EF* (the sample's longitudinal extrusion axis) for the ECAP and SCAP processes has been shown in Fig. 8(e). As observed from the diagrams, for both processes, the amount of strain from point *E* toward point *F* shows a little increase. The cause of this strain increase is the friction between the mold and sample in the outlet channel, which has also been demonstrated by El Mahallawy et al. (Ref 19). The strain increase along the longitudinal axis (from point *E* to *F*) has been higher for the SCAP process, which can be attributed to the passage of the sample through the twisted section of the mold at the outlet, which causes the friction to increase. Figure 8(b), (d), and (f) illustrates the results pertaining to hardness measurements along the *AB*, *CD*, and *EF*, respectively. As seen in the figure, the results related to the distribution of hardness in the sample have adequate agreement with those obtained from the simulation for effective strain; this indicates the direct influence of strain on hardness (Ref 21). Figure 9 depicts strain distributions in the longitudinal and transverse sections of the sample under the ECAP and SCAP processes. As observed in the figure, for the sample undergoing the SCAP process, the amount of strain is higher and the strain distribution is also more uniform. This fact has also been demonstrated in Fig. 8 by the strain-distance diagrams.

5. Conclusion

To achieve a more favorable outcome from the SPD methods, the two processes of ECAP and TE were combined in the intersecting section of the two mold channels, and the new method of SCAP was created. This method was evaluated through the finite element analysis and by performing practical experiments on pure aluminum. There is adequate correlation between the results obtained from the simulation and the experimental results for the applied loads in the SCAP process. There is also good agreement between the results of measured hardness and the strain results obtained from the simulation,

which indicates that the simulation results are correct. The results obtained via simulation for the imposed effective strains in the ECAP and SCAP indicate that the SCAP method, in addition to imposing a higher degree of strain, provides a more homogeneous distribution of strain inside the sample. This uniform distribution of strain is also validated in the transverse and longitudinal sections of the sample by means of hardness distribution measurements.

References

1. R.Z. Valiev and T.G. Langdon, Principles of Equal-Channel Angular Pressing as a Processing Tool for Grain Refinement, *Prog. Mater Sci.*, 2006, **51**, p 881–981
2. E.A. El-Danaf, M.S. Soliman, A.A. Almajid, and M.M. El-Rayes, Enhancement of Mechanical Properties and Grain Size Refinement of Commercial Purity Aluminum 1050 Processed by ECAP, *Mater. Sci. Eng. A*, 2007, **458**, p 226–234
3. A.P. Zhilyaev and T.G. Langdon, Using High-Pressure Torsion for Metal Processing: Fundamentals and Applications, *Prog. Mater. Sci.*, 2008, **53**, p 893–979
4. B. Han and Z. Xu, Microstructural Evolution of Fe–32%Ni Alloy During Large Strain Multi-Axial Forging, *Mater. Sci. Eng. A*, 2007, **447**, p 119–124
5. Y. Beygelzimer, V. Varyukhin, S. Synkov, and D. Orlov, Useful Properties of Twist Extrusion, *Mater. Sci. Eng. A*, 2009, **503**, p 14–17
6. D.H. Shin, J.J. Park, Y.S. Kim, and K.T. Park, Constrained Groove Pressing and its Application to Grain Refinement of Aluminum, *Mater. Sci. Eng. A*, 2002, **328**, p 98–103
7. Y. Saito, N. Tsuji, H. Utsunomiya, T. Sakai, and R.G. Hong, Ultra-Fine Grained Bulk Aluminum Produced by Accumulative Roll-Bonding (ARB) Process, *Scr. Mater.*, 1998, **39**, p 1221–1227
8. B. Mani, M. Jahedi, and M.H. Paydar, A Modification on ECAP Process by Incorporating Torsional Deformation, *Mater. Sci. A*, 2011, **528**, p 4159–4165
9. B. Talebanpour, R. Ebrahimi, and K. Janghorban, Microstructural and Mechanical Properties of Commercially Pure Aluminum Subjected to Dual Equal Channel Lateral Extrusion, *Mater. Sci. Eng. A*, 2009, **527**, p 141–145
10. K. Nakashima, Z. Horita, M. Nemoto, and T.G. Langdon, Influence of Pressing Speed on Microstructural Development in Equal-Channel Angular Pressing, *Metall. Mater. Trans. A*, 1999, **30**, p 1989–1997
11. X. Ma, M.R. Barnett, and Y.H. Kim, Forward Extrusion Through Steadily Rotating Conical Dies. Part I: Experiments, *Int. J. Mech. Sci.*, 2004, **46**, p 449–464

12. A.P. Shpak, V.N. Varyukhin, V.I. Tkatch, V.V. Maslov, Y.Y. Beygelzimer, S.G. Synkov, V.K. Nosenko, and S.G. Rassolov, Nanostructured $Al_{86}Gd_6Ni_6Co_2$ Bulk Alloy Produced by Twist Extrusion of Amorphous Melt-Spun Ribbons, *Mater. Sci. Eng. A*, 2006, **425**, p 172–177

13. S.A.A. Akbari Mousavi, Sh. Ranjbar Bahadori, and A.R. Shahab, Numerical and Experimental Studies of the Plastic Strains Distribution Using Subsequent Direct Extrusion After Three Twist Extrusion Passes, *Mater. Sci. Eng. A*, 2010, **527**, p 3967–3974

14. D. Orlov, Y. Beygelzimer, S. Synkov, V. Varyukhin, N. Tsuji, and Z. Horita, Plastic Flow, Structure and Mechanical Properties in Pure Al Deformed by Twist Extrusion, *Mater. Sci. Eng. A*, 2009, **519**, p 105–111

15. V.M. Segal, Severe Plastic Deformation: Simple Shear Versus Pure Shear, *Mater. Sci. Eng. A*, 2002, **338**, p 331–344

16. R. Kocicha, M. Greger, M. Kursa, I. Szurman, I. Szurman, and A. Machackova, Twist Channel Angular Pressing (TCAP) as a Method for Increasing the Efficiency of SPD, *Mater. Sci. Eng. A*, 2010, **527**, p 6386–6392

17. N. Bay, Friction Stress and Normal Stress in Bulk Metal-Forming Processes, *J. Mech. Work. Technol.*, 1987, **14**, p 203–223

18. W. Wei, A.V. Nagasekhar, G. Chen, Y. Tick-Hon, and K.X. Wei, Origin of Inhomogenous Behavior During Equal Channel Angular Pressing, *Scr. Mater.*, 2006, **54**, p 1865–1869

19. N. El Mahallawy, F.A. Shehata, M. Abd El Hameed, M. Ibrahim Abd El Aal, and H.S. Kim, 3D FEM Simulations for the Homogeneity of Plastic Deformation in Al–Cu Alloys During ECAP, *Mater. Sci. Eng. A*, 2010, **527**, p 1404–1410

20. Y. Iwahashi, J. Wang, Z. Horita, M. Nemoto, and T.G. Langdon, Principle of Equal-Channel Angular Pressing for the Processing of Ultra-Fine Grained Materials, *Scr. Mater.*, 1996, **35**, p 143–146

21. O.F. Sonmez and A. Demir, Analytical Relations Between Hardness and Strain for Cold Formed Parts, *J. Mater. Process. Technol.*, 2007, **186**, p 163–236